

Internal Report

DESY D3-52

April 1984

SYNCHROTRON RADIATION  
IN THE PETRA TUNNEL

H. Dinter

Eigentum der	DESY	Bibliothek
Property of		library
Zugang:	- 7. MAI 1984	
Accessions:		
Leihfrist:	/	
Loan period:	/ days	

**DESY behält sich alle Rechte für den Fall der Schutzrechtserteilung und für die wirtschaftliche Verwertung der in diesem Bericht enthaltenen Informationen vor.**

**DESY reserves all rights for commercial use of information included in this report, especially in case of filing application for or grant of patents.**

**"Die Verantwortung für den Inhalt dieses Internen Berichtes liegt ausschließlich beim Verfasser"**

**SYNCHROTRON RADIATION IN THE PETRA TUNNEL**

**Internal Report D03-52**

**April 1984**

**H. Dinter**

## ABSTRACT

A collection of results of measurements of absorbed doses due to synchrotron radiation is presented and compared with calculations.

**CONTENTS**

1.0 INTRODUCTION ..... 1

2.0 MEASUREMENTS ..... 2

3.0 CALCULATIONS ..... 5

4.0 RESULTS ..... 6

4.1 Horizontal dose distributions ..... 6

4.2 Vertical dose distributions ..... 8

4.3 Isodose curves ..... 9

4.4 Longitudinal dose distributions ..... 9

4.5 Absorbed doses as function of beam energies ..... 12

4.6 Absorbed doses behind lead, and effective energies ..... 12

4.7 Absorbed energy in components ..... 17

5.0 SUMMARY ..... 20

6.0 LITERATURE ..... 21

LIST OF ILLUSTRATIONS

Figure 1. Cross section of the PETRA tunnel . . . . . 3  
Figure 2. Geometry of a dipole magnet used for calculations . . . . . 4  
Figure 3. Horizontal dose distributions in beam height . . . . . 7  
Figure 4. Vertical dose distributions before a dipole magnet . . . . . 8  
Figure 5. Distribution of isodoses . . . . . 10  
Figure 6. Absorbed doses within the gap of a dipole magnet . . . . . 11  
Figure 7. Doses in beam height . . . . . 13  
Figure 8. Doses in front of a dipole magnet . . . . . 14  
Figure 9. Doses below a dipole magnet . . . . . 15  
Figure 10. Doses at the tunnel wall . . . . . 16  
Figure 11. Table 1 . . . . . 17  
Figure 12. Energy absorbed in a dipole magnet . . . . . 19

## 1.0 INTRODUCTION

Since 1981 the beam energy of the storage ring PETRA was increased from 17 to nearly 23.5 GeV. The energy emitted as synchrotron radiation depends strongly on the energy of the accelerated particles. Therefore, the rates of the absorbed doses due to synchrotron radiation have increased as well. A high radiation level in the tunnel however, causes damages of accelerator components located near the radiation source or being especially sensitive to ionizing radiation.

We measured the absorbed dose at a series of beam energies between 17.3 and 22.8 GeV in the bent ring tunnel, and in addition we performed calculations of absorbed doses in the region between 17.5 and 30 GeV, in order to be able to predict absorbed doses, and to improve the shielding, if necessary.

•  
This report is a compilation of the results of these activities within the last 2 years. Parts of the data already have been published in ref.1 and 2, but the experimental data of ref.1 only extend up to 17 GeV. The calculated doses reported in ref.2 were recalculated and limits of uncertainties due to the statistic nature of the Monte Carlo procedures are added. At 9 different beam energies the calculated doses now can be checked against measured ones.

## 2.0 MEASUREMENTS

All dose measurements were performed using RPL-glass dosimeters. In consequence, all doses quoted in this report are doses of absorbed energy in glass. Because of its mean atomic data (mean atomic weight =  $25 \text{ g}\cdot\text{mol}^{-1}$ ; mean atomic number = 12; density =  $2.6 \text{ g}\cdot\text{cm}^{-3}$ ), and its absorption coefficient, glass may be regarded as an accelerator component like aluminium. A detailed description of the methods of dose measurements can be found in ref.1 and 3.

The encapsulated dosimeters were fixed equidistantly on strings spanned across the tunnel, and along the wall of the tunnel and the dipole magnets (indicated in Figure 1 on page 3).

The horizontal and the vertical dosimeter strings (lines H, V1, V2, V3) were positioned in the middle of a dipole magnet located in the middle of the tunnel arc between the experimental halls East and Southeast of PETRA.

The synchrotron radiation hits the vacuum chamber not only within the dipole magnet, but because of its very small emission angle also within the small straight section between dipole and sextupole magnet. There, the arrangement of the materials surrounding the beam and shielding the synchrotron radiation is quite different from that in the middle of a dipole. Therefore, another horizontal string of dosimeters was spanned between such a straight section and the tunnel wall, to find out the differences of dose distributions of both positions.

One of the longitudinal strings were fixed at the tunnel wall in beam height, opposite to the magnet gap, covering the length of one "magnetic cell", i.e. ranging from the middle of one dipole magnet to the middle of the next one.

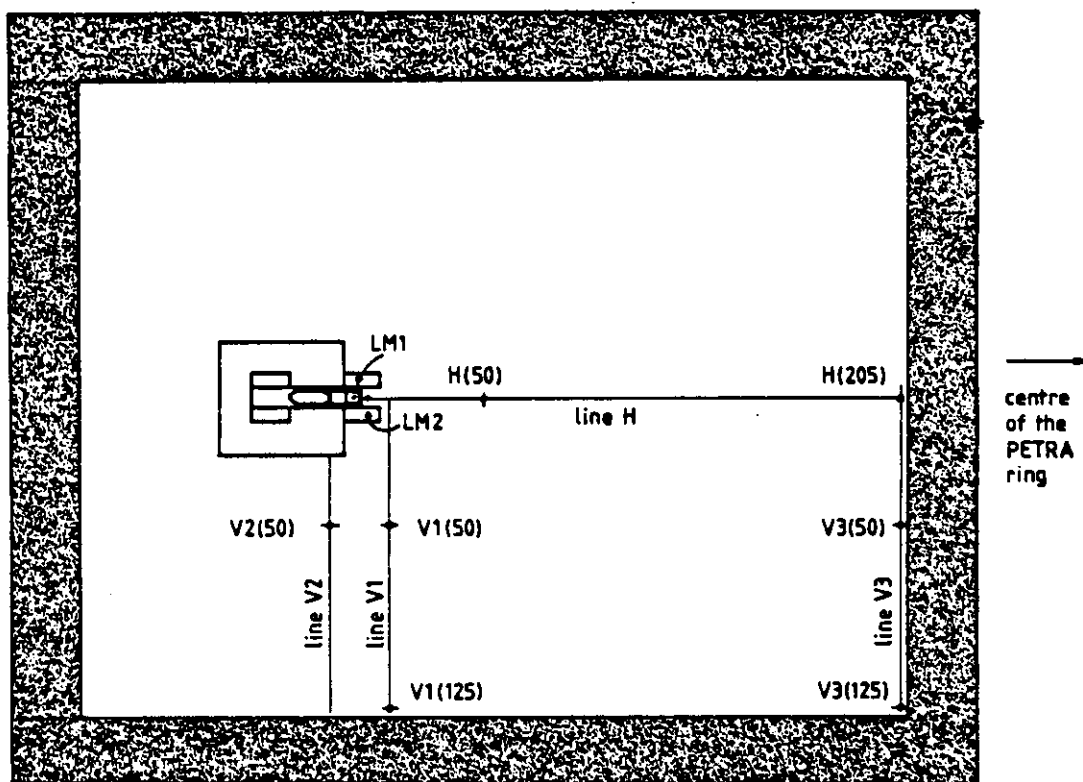
Two other strings (LM1 and LM2), were mounted within the gap of a dipole magnet, one before, and the other behind 3 mm of lead, shielding all the dipole gaps (Figure 1 on page 3 and Figure 2 on page 4).

At the highest energy of 22.8 GeV, two additional measurements were performed: At some points on the floor, at the wall, and within the dipole gap the attenuation of the doses by 4 mm of lead surrounding the dosimeters was studied.

For one position at the wall and in beam height the decrease of the doses behind lead from 1 up to 10 mm was investigated, in steps of 1 mm, in order to get an idea of the effective energy of the multiply scattered photons of the synchrotron radiation.

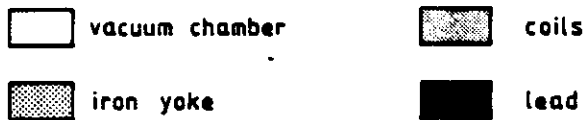
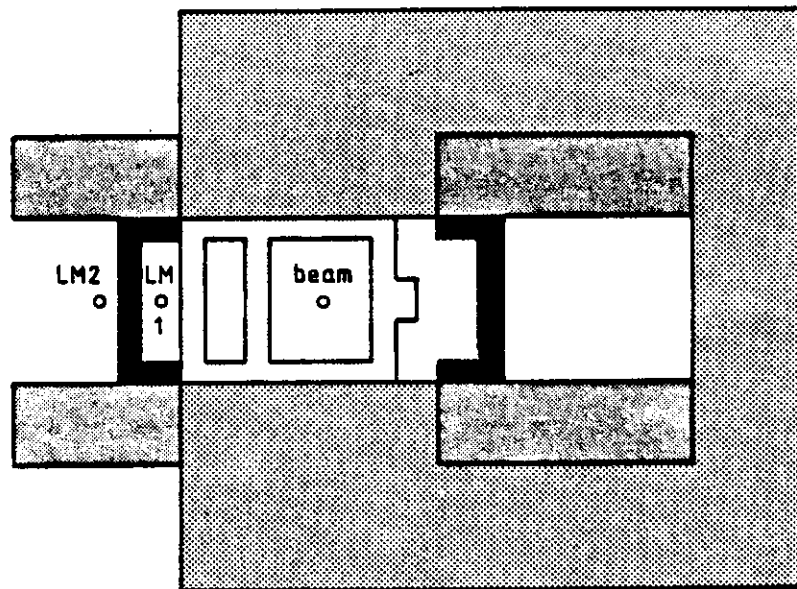


All measured doses were normalized to a charge of 0.1 Ah of accelerated particles, both electrons and positrons. The accuracy of this normalization should be better than 10 %. At all energies this amount of 0.1 Ah was reached within 14 hours ( $\pm 10\%$ ), ramping, injection time, and other breaks excluded.



37156

Figure 1. Cross section of the PETRA tunnel: The tunnel is cut amidst a dipole magnet. The positions of 1 horizontal and 3 vertical strings loaded with dosimeters are indicated as lines H, V1, V2, V3. The solid points are positions used for dose calculations as a function of beam energies. LM1, LM2 are longitudinal strings behind and before the 3 mm-lead shield in the magnet gap.



not in scale

Figure 2. Geometry of a dipole magnet used for calculations: Rectangular approach to the cross section of a PETRA dipole magnet (the proportions are not in scale).

### 3.0 CALCULATIONS

The calculations were performed using the Monte Carlo program system EGS-version3 (ref.4). The photons of the synchrotron radiation are transported by this code in an arrangement of materials which represent a rectangular approach to the cross section of the tunnel, cut just in the middle of a dipole magnet (for the calculations of the doses in the tunnel), see Figure 1 on page 3, and to the cross section of a dipole magnet (for calculations of deposited energies in the dipole components), see Figure 2 on page 4.

The values of the absorbed doses (in glass) are obtained from the corresponding kerma values, assuming an equilibrium of secondary electrons. The kerma itself is calculated by means of the energies of the photons entering a certain air region, and by the mass energy absorption coefficient of RPL-glass. The techniques used are just the same as described in ref.1.

If the number of photons entering a geometrical region is low (occurring especially at low beam energies), it is difficult to obtain a dose value of a reasonable significance. Therefore, at each beam energy a series of long-running jobs were submitted to the computer (10 minutes of CPU-time per job at a IBM 3081). The results of each job were regarded as a statistical event. The doses of each region were averaged over all completed jobs, and standard deviations were calculated. If the number of jobs is low, the standard deviations show severe jumps or oscillations when they are plotted as a function of the number of the evaluated jobs. Only at a higher number of jobs, depending on the number of particles entering a region of interest, the standard deviation becomes constant for this region. After becoming constant for all regions, and lasting constant for 4 or 5 jobs, the calculational procedure was stopped. In this way one may be sure that the standard deviation has reached a meaningful value.

When the number of photons in a region is extremely low, standard deviations of several hundred percent can occur. Therefore, in such cases the uncertainties are expressed as factors (factor of 2 means a 100 %-standard deviation etc.).

The lines connecting the end-points of corresponding standard deviations are called the "one-standard deviation limits" of the calculations.

## 4.0 RESULTS

### 4.1 HORIZONTAL DOSE DISTRIBUTIONS

The horizontal distribution of absorbed doses in the middle of a dipole magnet (line H in Figure 1 on page 3) is shown in Figure 3 on page 7 for 3 beam energies, both calculated and measured values.

Next to the vacuum pipe the calculated doses are systematically higher than the measured ones with an increasing tendency to higher beam energies. However at distances above around 70 cm, the measured doses match fairly well within the one-standard deviation limits of EGS.

The horizontal dose distribution between the wall and a distance of 50 cm from the beam pipe, measured in the middle of a small straight section give up to 50 % higher values than measured at the dipole centre. Below this distance of 50 cm, the doses become higher than the corresponding of line H, increasing up to a factor of 10 when approaching to the pipe.

The range where the synchrotron radiation emerging from a dipole magnet and hitting the vacuum chamber extends beyond the dipole magnet into the small straight section, because of the small angle between the orbit and the tangential direction of the emitted synchrotron radiation.

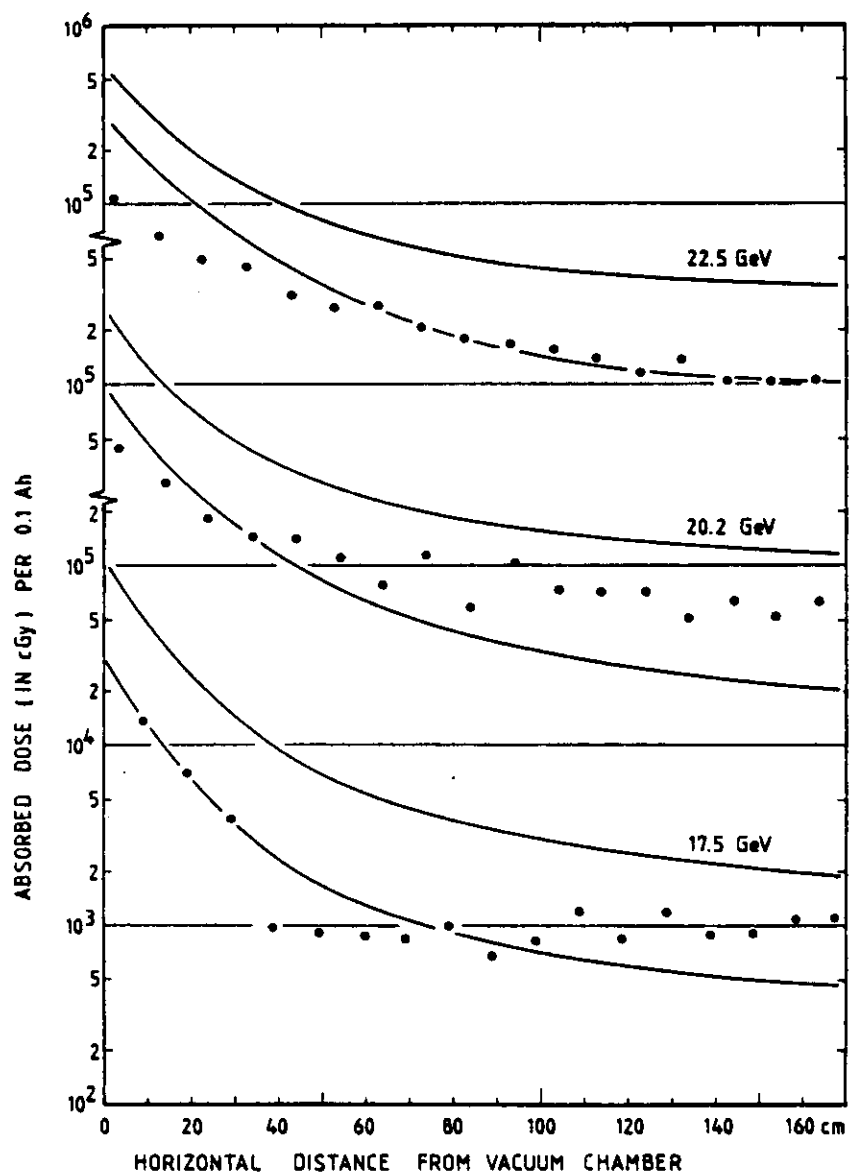
The absorbed dose measured in the tunnel at beam height originates from radiation scattered at the vacuum tube, especially at the nose around the cooling channel. Therefore, the horizontal dose distributions, both in the middle of a dipole and of a small straight section should be the same. This is confirmed by an EGS-calculation using a tunnel geometry (the same as used for Figure 3 on page 7), but without the magnet yoke. The measured enhancement of the doses next to the beam pipe is due to the unshielded flansh of the bellow.

The different arrangement of materials around the vacuum chamber at the small straight section and at the position of a dipole magnet only takes effect to doses well below and above beam height.

### 4.2 VERTICAL DOSE DISTRIBUTIONS

In Figure 4 on page 8 the curves for vertical dose distribution of line V1 (see Figure 1 on page 3) are given, again amidst a dipole magnet.

These doses are lower than those of the horizontal line. Therefore, the calculational uncertainties are rather large, especially at low energies.



37154

Figure 3. Horizontal dose distributions in beam height: Measured and calculated values at 3 beam energies along line H of Figure 1 on page 3. The solid symbols represent measured data; the lines show the one-standard deviation limits of the calculations.

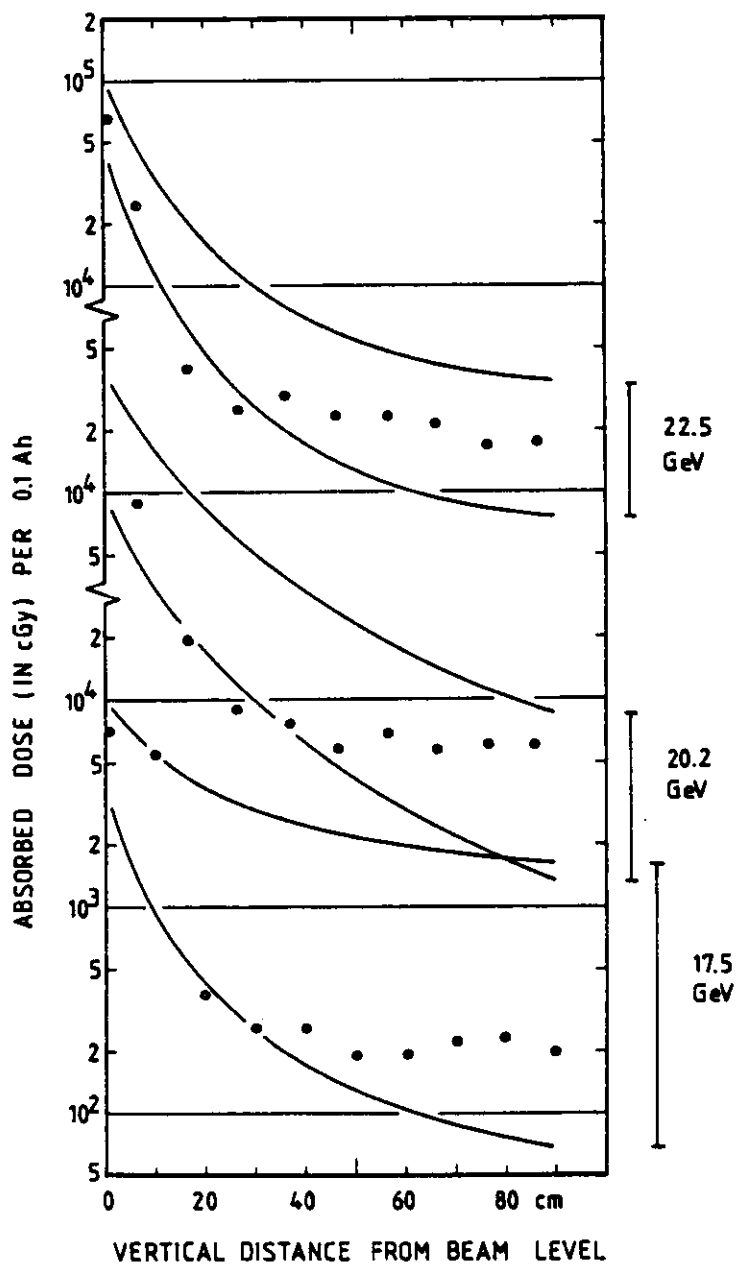


Figure 4. Vertical dose distributions before a dipole magnet: Measured and calculated values at 3 beam energies along line V1 of Figure 1 on page 3. The solid symbols represent measured data; the lines show the one-standard deviation limits of the calculations.

Nevertheless, the agreement between the centre of the area of uncertainty and the measured values is better than a factor of 2.

### 4.3 ISODOSE CURVES

At the highest energy, at 22.8 GeV, a lot of vertical and horizontal dosimeter strings were spanned all over the tunnel cross section (which are not shown in detail in the figures). From the results, curves of isodoses are drawn, and presented in Figure 5 on page 10. This figure gives an impression of the spacial dose distribution. A relatively small dose gradient is found in the lower and the higher parts of the tunnel, leading to the approximation of a "rather uniform dose distribution" throughout the tunnel, excepting the region in beam height.

### 4.4 LONGITUDINAL DOSE DISTRIBUTIONS

The distribution of the absorbed doses in longitudinal direction was studied in 3 ways:

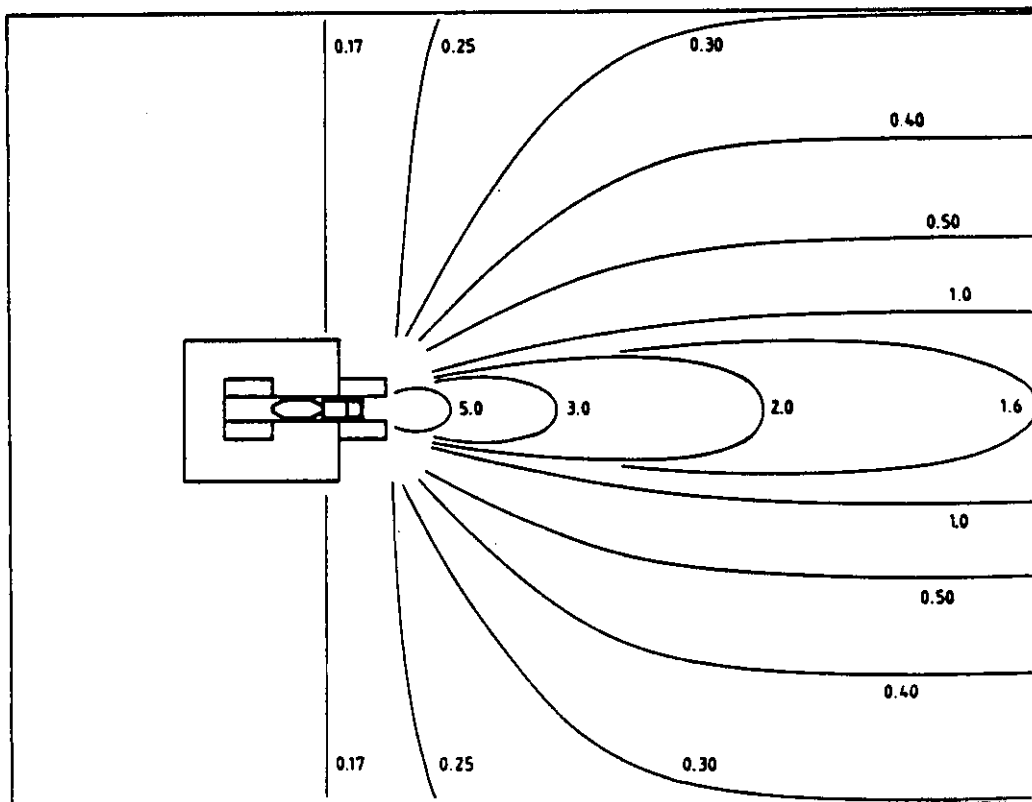
Dosemeters fixed at the wall in beam height between the centres of 2 dipole magnets show a nearly uniform distribution (within  $\pm 10\%$  from the average), excepted a 50 %-enhancement opposite to the small straight section, due to the bad shielding conditions near the bellow, mentioned above. The measured values agree well with the dose at the end-point of line H (point H(205) in Figure 1 on page 3 and Figure 7 on page 13).

Two other strings charged with dosimeters have been spanned behind and before the 3 mm-lead shield within the magnet gap (lines LM1 and LM2 in Figure 1 on page 3 and Figure 2 on page 4). All the measured doses of each line centre around an average value with a standard deviation of 20 %. Therefore, these values are plotted as bars (at 22.8 GeV), together with the older values of ref.1 at 17 GeV in Figure 6 on page 11.

In addition the calculated doses are shown as a function of the beam energy. For LM1 (the line next to the vacuum chamber, behind the lead) the measured doses are approximately a factor of 2 lower than the calculated ones, whereas the agreement for line LM2 (before the lead shield, at the tunnel side) is fairly good. From the curve at the bottom of the figure, the attenuation of absorbed doses by 3 mm of lead can be found, amounting to a factor of 100 at 22.8 GeV.

In order to be sure that the position in the tunnel where the measurements were carried out is not an exceptional one, but that the doses are

similar at corresponding positions all over the tunnel arc, a measurement was performed along a complete octant of the PETRA ring. Dosimeters have been fixed at the tunnel wall in beam height, opposite to each quadrupole magnet. The averaged doses measured at 22.05 GeV amount to  $(2.7 \pm 1.0) \cdot 10^4$  cGy/0.1 Ah (which agrees well with position H(205) in Figure 1 on page 3 and Figure 7 on page 13)<sup>1</sup>. This means that the isodose curves of Figure 5 continues longitudinally like hoses all over the



37152

Figure 5. Distribution of isodoses: measured absorbed doses in the PETRA tunnel at a beam energy of 22.8 GeV. The figures are given in units of  $10^4$  cGy/0.1 Ah.

<sup>1</sup> 1 cGy = 1 rad



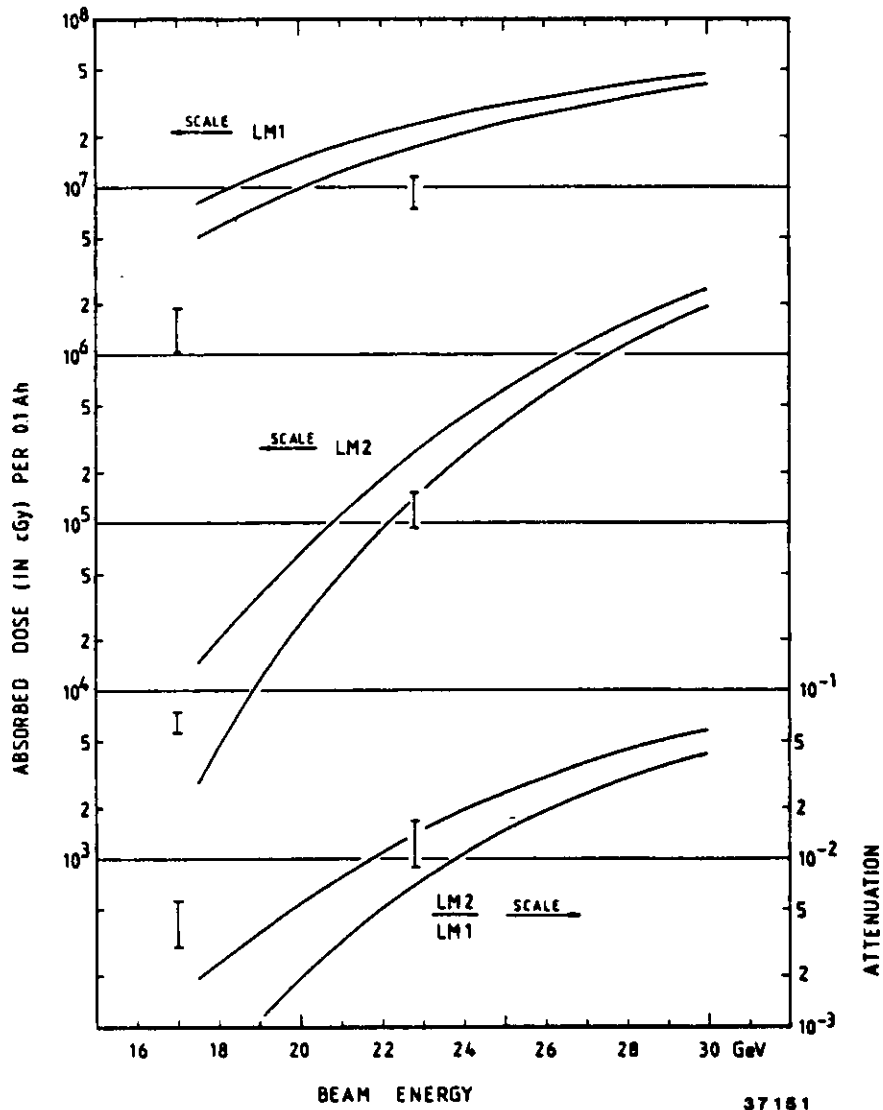


Figure 6. Absorbed doses within the gap of a dipole magnet: LM1 means the position behind the lead shield on the side of the vacuum pipe; LM2 means the position before the shield on the tunnel side (see Figure 1 on page 3 and Figure 2 on page 4). The bars give averaged experimental data; the lines show the one-standard deviation limits of the calculated values as a function of the beam energy.

bent part of the tunnel with some disturbances around the small straight sections.

#### 4.5 ABSORBED DOSES AS FUNCTION OF BEAM ENERGIES

Some positions in the tunnel cross section considered to be important for installations were selected, in order to study the absorbed doses at these points as a function of the beam energy. These positions are indicated in Figure 1 on page 3. They are marked by the character of the string they belong to, and in brackets by the distance from the vacuum pipe (for the horizontal line H), and from the beam height downward (for the vertical lines V1, V2, and V3), respectively.

Figure 7 on page 13 up to Figure 10 on page 16 show the measured doses compared with the one-standard deviation limits of the calculations. All measured doses of the selected positions agree well within these limits.

#### 4.6 ABSORBED DOSES BEHIND LEAD, AND EFFECTIVE ENERGIES

At some other interesting positions, dosimeters surrounded by 4 mm of lead have been exposed. The results and the corresponding effective energies of the photons are listed in Figure 11 on page 17. The least attenuation was found immediately behind the installed lead shield, within the magnet gap. Moving from the gap to the tunnel wall, then downward to the floor, and on the floor backward until a position below the magnet, the attenuation becomes stronger, and the effective energy becomes softer, due to the increasing amount of scattered radiation contributing to the absorbed dose.

At the wall in beam height, the attenuation in lead was investigated in more detail by surrounding dosimeters by lead with a thickness of 1 up to 10 mm, in steps of 1 mm. The result is a nearly pure exponential attenuation curve between 1 and 10 mm giving an effective energy of about 300 keV independent from the lead thickness. This is in qualitative agreement with the spectra previously calculated in ref.2.

#### 4.7 ABSORBED ENERGY IN COMPONENTS

So far absorbed doses in glass were considered as they may be measured in air regions of the PETRA tunnel. Another complex of questions is that of the doses absorbed within the accelerator components themselves. However, measurements are difficult to realise, and are not yet performed.

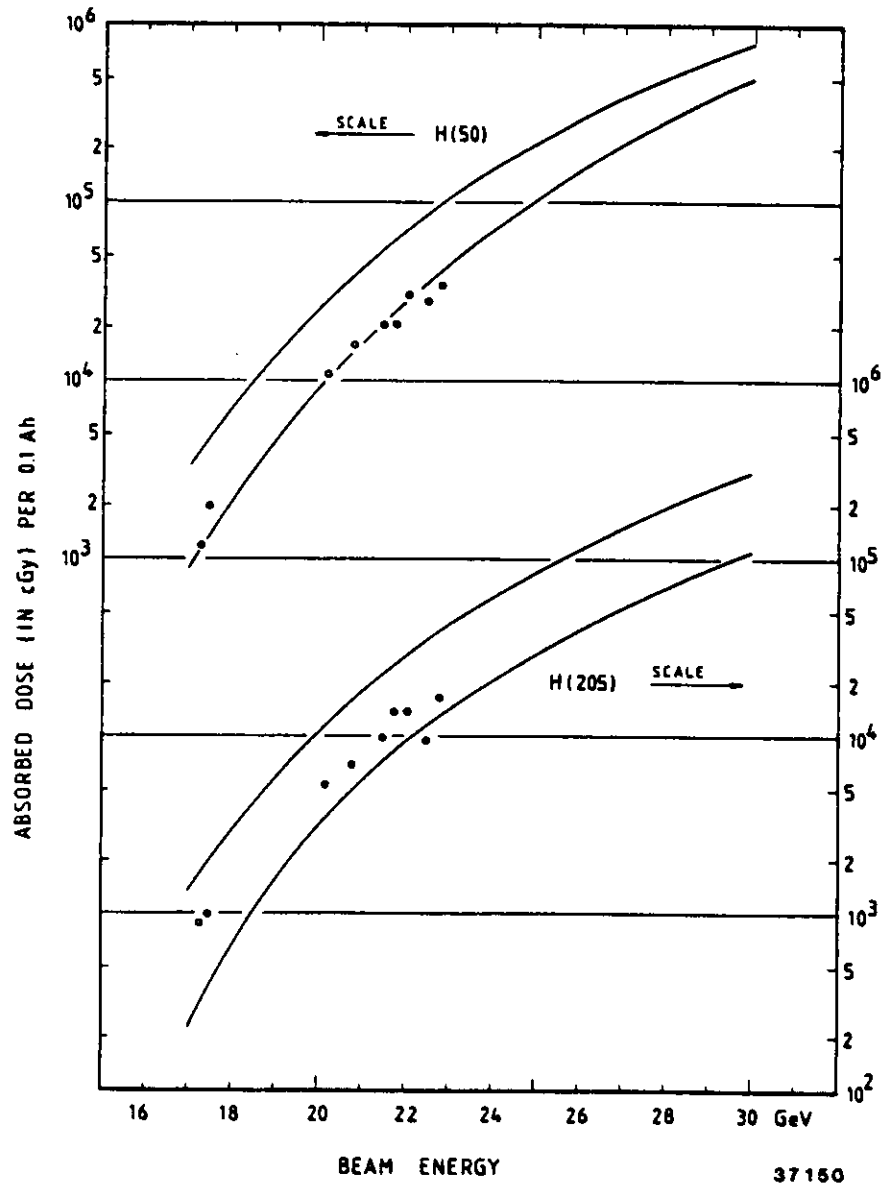


Figure 7. Doses in beam height: Dose values for 2 positions are given as a function of beam energy, one at a distance of 50 cm from the beam pipe (H(50)), and another at the wall (H(205)). See Figure 1 on page 3. The dots represent the measured doses, whereas the lines indicate the one-standard deviation limits of the calculations.

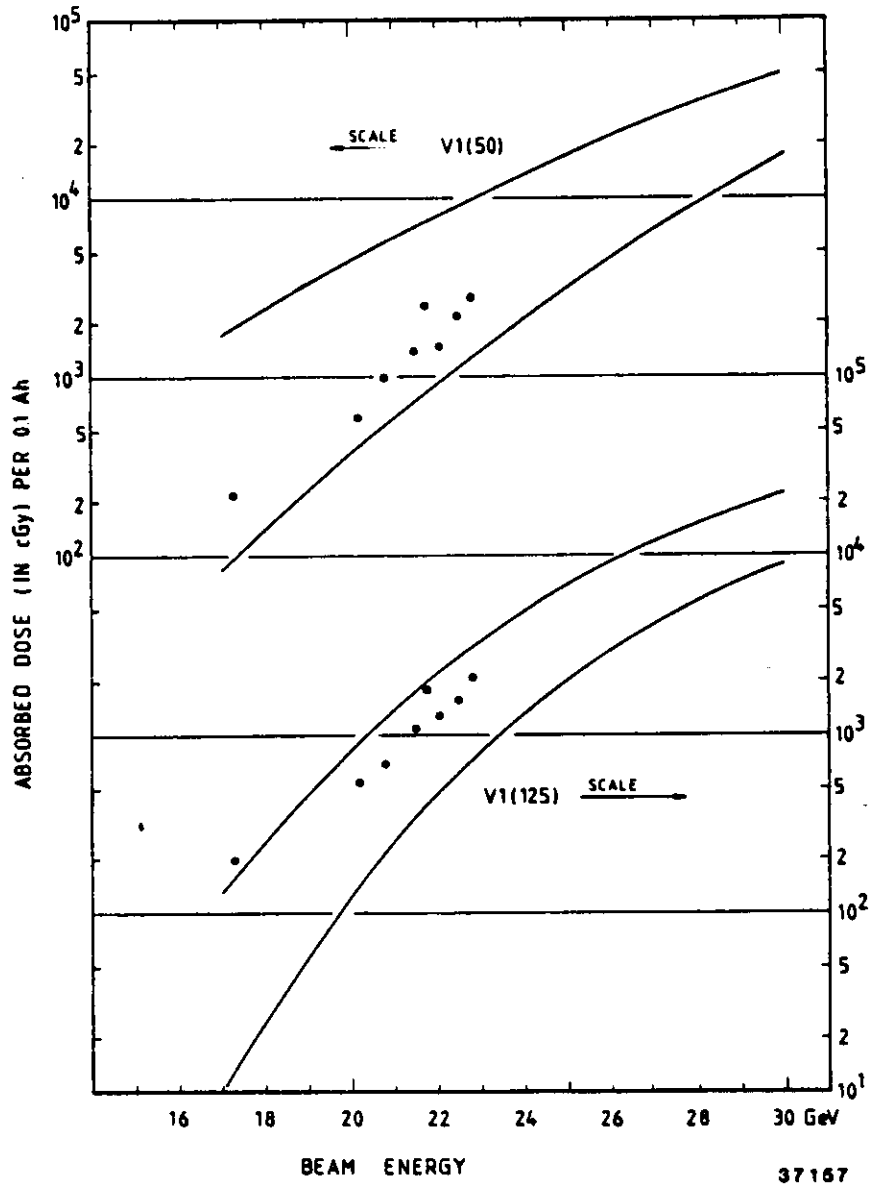


Figure 8. Doses in front of a dipole magnet: Dose values for 2 positions are given as a function of energy, one at a distance of 50 cm below beam height (V1(50)), and another on the floor (V1(125)). See Figure 1 on page 3. The dots represent the measured doses, whereas the lines indicate the one-standard deviation limits of the calculations.

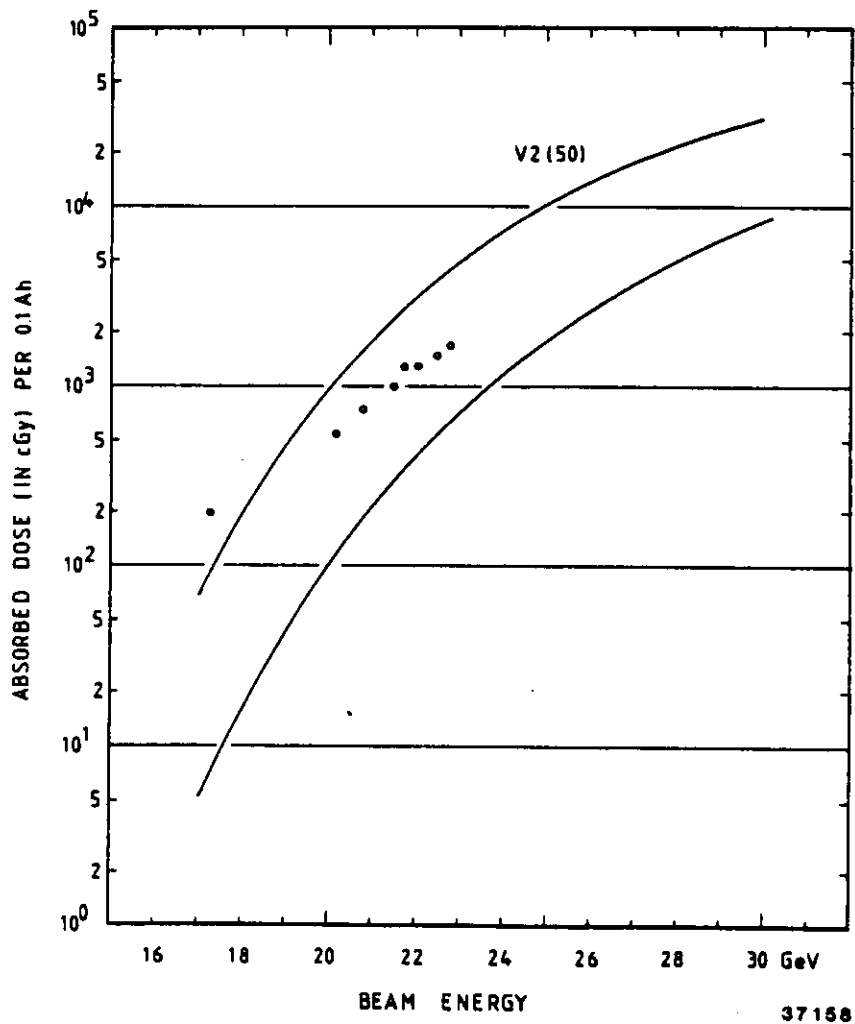


Figure 9. Doses below a dipole magnet: Dose values for 2 positions are given as a function of energy, one at a distance of 50 cm below beam height (V2(50)), and another on the floor (V2(125)). See Figure 1 on page 3. The dots represent the measured doses, whereas the lines indicate the one-standard deviation limits of the calculations.

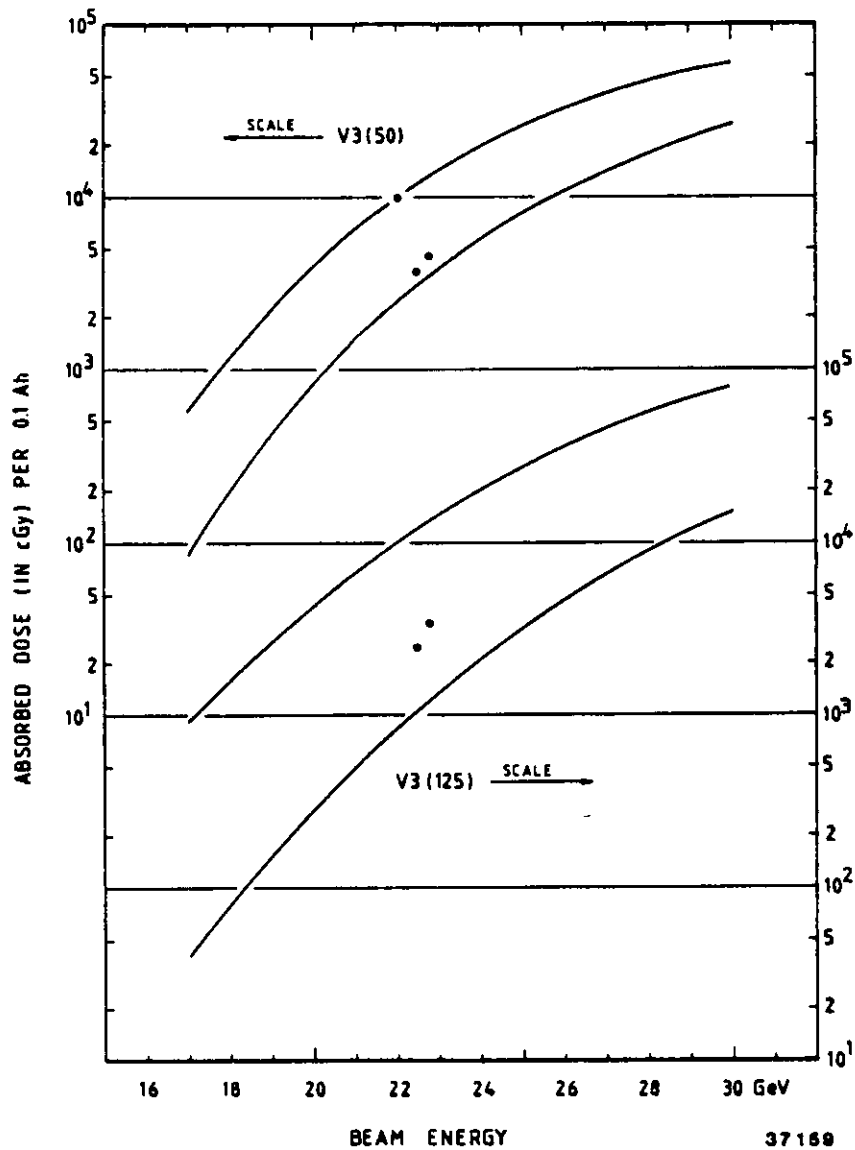


Figure 10. Doses at the tunnel wall: Dose values for 2 positions are given as a function of energy, one at a distance of 50 cm below beam height (V3(50)), and another on the floor (V3(125)). See Figure 1 on page 3. The dots represent the measured doses, whereas the lines indicate the one-standard deviation limits of the calculations.

Position	Attenuation	Eff. Energy in keV
Magnet gap, before shield	0.45	360.
Tunnel wall, beam height	0.20	275.
Tunnel wall, floor	0.05	195.
Floor, below dipole magnet	0.02	175.

Figure 11. Table 1: Attenuation of absorbed doses by surrounding the dosimeters with 4 mm of lead, at different positions, and effective energies derived from this attenuations.

But the EGS-code has proved to be a useful tool for predicting absorbed doses, and will be well suited for calculating absorbed energies in components.

In Figure 12 on page 19 the results for different components of a dipole magnet are plotted against the beam energy using the geometry given in Figure 2 on page 4. The absorbed energies are normalized to the total incoming energy. The lines again represent the one-standard deviation limits of the EGS-calculations.

The plotted absorbed energy fractions mean an average value over one distinct accelerator component and do not give any indication of critical regions like edges or corners near the radiation source.

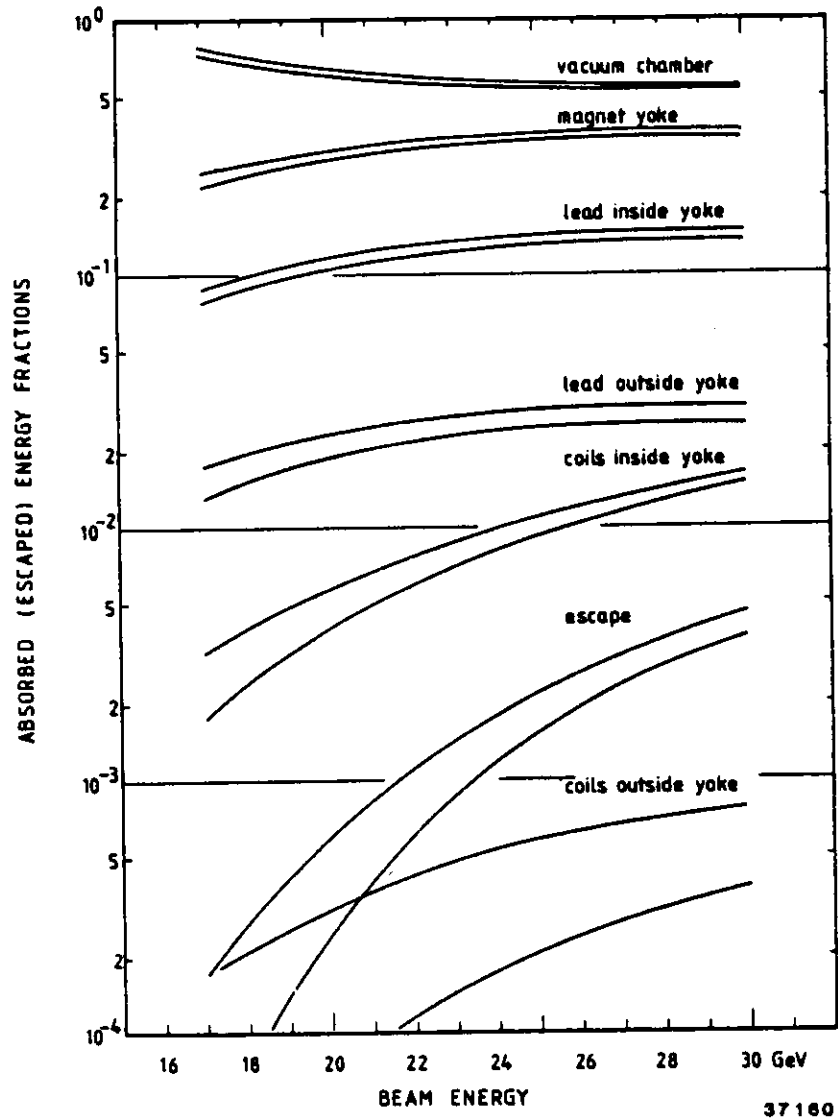


Figure 12. Energy absorbed in a dipole magnet: Energy fractions absorbed by the main components of a PETRA dipole magnet, and escaped through the gap of this magnet are calculated as a function of beam energy.



## 5.0 SUMMARY

Measurements of the absorbed doses due to scattered synchrotron radiation were performed in the bent part of the PETRA tunnel in the energy region between 17.3 and 22.8 GeV. The EGS-code was used for the calculation of absorbed doses in air regions in the tunnel, and of absorbed energy fractions in the components of a dipole magnet as well. In addition limits of uncertainties for these calculations are given. All calculated data agree with the measured ones within a factor 2 to 3.

## 6.0 LITERATURE

1. H.Dinter, K.Tesch, C.Yamaguchi:

Absorbed radiation dose due to synchrotron radiation  
in the storage ring PETRA

Nucl. Instr. Meth. 200 (1982) 437

2. H.Dinter:

Synchrotron radiation in the PETRA tunnel for beam  
energies up to 30 GeV

Internal Report DESY D03-42 (1982)

3. K.Tesch:

Measuring absorbed doses between  $10^{-2}$  and  $10^8$  Gy  
with a single glass dosimeter

Rad. Prot. Dosimetry 6 (1984) 347

4. R.L.Ford, W.R.Nelson:

The EGS code system

SLAC Report No. 210 (1978)

### Acknowledgement

I am grateful to all members of the group D3 who prepared and evaluated hundreds of doseimeters.